Wired Up: Interconnecting Two-Dimensional Materials with One-Dimensional Atomic Chains

Youmin Rong and Jamie H. Warner*

Department of Materials, University of Oxford, Parks Road, Oxford OX1 3PH, United Kingdom

ABSTRACT Atomic wires are chains of atoms sequentially bonded together and epitomize the structural form of a one-dimensional (1D) material. In graphene, they form as interconnects between regions when the nanoconstriction eventually becomes so narrow that it is reduced to one atom thick. In this issue of *ACS Nano*, Cretu *et al.* extend the discovery of 1D atomic wire interconnects in two-dimensional (2D) materials to hexagonal boron nitride. We highlight recent progress in the area of 1D atomic wires within 2D materials, with a focus on their atomic-level structural analysis using aberration-corrected transmission electron microscopy. We extend this discussion to the formation of nanowires in transition metal dichalcogenides under similar electron-beam irradiation conditions. The future outlook for atomic wires is considered in the context of new 2D materials and hybrids of C, B, and N.

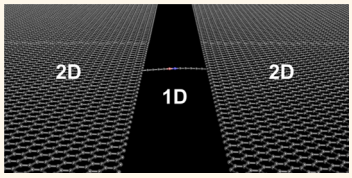

Miniaturization of individual elements in electronic circuits eventually leads to the scenario of single-atom transistors, atomic point contacts, and atomic one-dimensional (1D) chains. Building ultrasmall electronic devices, such as transistors, based on a silicon platform has demonstrated the state-of-the-art in bottom-up nanofabrication with atomic-level precision.[1] However, extending bottom-up strategies to the large-scale arrays required for generating complex circuitry is extremely challenging to implement. One example of this is the implementation of carbon nanotubes (CNTs) in large-scale electronics, where the major challenge is to grow CNTs in exactly the right location on a substrate. A similar problem exists for bottom-up fabricated graphene nanoribbons using molecular precursors on substrates.[2] The large-scale bottom-up fabrication of atomic wires made rapid progress through the use of CNT interiors as a template to control growth. This has resulted in linear carbon chains, metal wires, and, recently, ionic wires formed within the 0.7−2 nm hollow inner core of the CNT.[3−5] However, a major challenge for further progress using template bottom-up growth within CNTs is the effective removal of the nanotube host, while maintaining stabilization of the linear atomic chain.

Top-down methods are another option for the fabrication of 1D atomic-scale structures. Two-dimensional (2D) materials are highly amenable to top-down fabrication because they only require controlled patterning in 2D, rather than three dimensions (3D), as required for silicon processing technology. General approaches for top-down patterning use electron-beam lithography and photolithography methods to generate nanostructures down to ∼10 nm. Direct electron-beam irradiation of 2D materials performed *in situ* within a transmission electron microscope has opened up new insights into the fabrication of structures down to the atomic level through controlled sputtering or irradiation-induced restructuring with simultaneous real-time imaging. Aberration-corrected transmission electron microscopy (AC-TEM) has improved spatial resolution, which can be extended even further by monochromation of the electron source to provide single-atom imaging capabilities of low *Z* number materials such as carbon.[6] With AC-TEM, a focused electron beam can now reach diameters as small as ∼0.1 nm, enabling the possibility of single-atom manipulation. If the energy of the electrons within the electron beam in an AC-TEM is close to the threshold for sputtering, then atoms are removed from the sample and nanosculpting begins. For materials like graphene, this threshold is between 60 and 80 keV. If the energy of electrons in the beam is much higher than this, then graphene is rapidly deformed through the

* Address correspondence to jamie.warner@materials.ox.ac.uk.

Published online December 04, 2014
10.1021/nn5065524

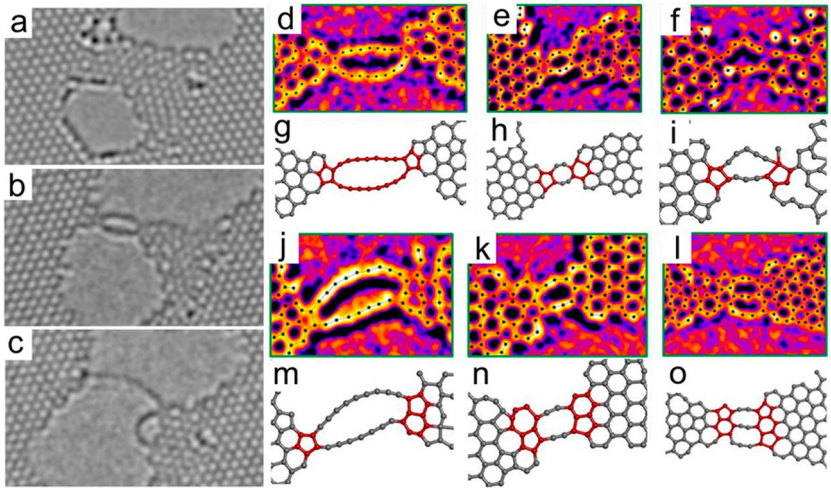

Figure 1. Double C atomic wire. (a–c) Sequence of AC-TEM images of graphene under 80 kV electron-beam irradiation showing the formation process of linear carbon atomic wires. (d–f) AC-TEM images (false color) of different double carbon chain interconnects bonded to the same aromatic ring on both sides of graphene. (g–i) Atomic models for the AC-TEM images shown in (d–f), respectively. (j–l) AC-TEM images (false color) of different double carbon chain interconnects that bond to multiple aromatic rings at the edge. (m–o) Atomic models for the AC-TEM images shown in (j–l), respectively.

introduction of defects and holes across large areas.

Linear Carbon Wires in Graphene. Some of the early experiments on electron-beam sputtering of CNTs revealed that linear carbon chains formed as the penultimate stage before nanotube breakage.[7] More recently, research has focused on carbon chains that form in graphene irradiated by the electron beam.[8,9] Electron-beam irradiation at an accelerating voltage of 80 kV typically forms holes within the sheet, and when two of these holes meet, a nanoconstriction is formed, as shown in Figure 1a. As this nanoconstriction further thins out by atom loss, it leads to the formation of a double carbon chain system (Figure 1b). Eventually, one of the two chains breaks, leaving a single carbon chain interconnecting two regions of graphene (Figure 1c). The interesting aspect about this formation process is that it never produces a linear sequence of fused aromatic rings, with pentacene-like form, but instead leads to the split double chain structure, where each chain is highly curved. It is also not very dependent upon the starting quality of 2D carbon material, with amorphous 2D carbon also showing similar linear carbon chain formation. The double carbon chain can have attachment points to the same aromatic ring on either side of the graphene, as shown in Figure 1d–i. In this case, the attachment point is often a pentagon, rather than a hexagonal ring. In order to maintain the 120° angle for sp^2 bonding in the pentagonal attachment site, the chains are required to be curved. Sometimes, the double carbon chains are attached to two aromatic rings (shown in Figure 1j–o), and in these cases, the degree of curvature in the linear chains is less and the two rings are often a hexagon and pentagon combination.

The specific bonding structure of the linear carbon chains formed within graphene has not been directly confirmed by atomic resolution imaging and remains an open question. There are two main types of linear carbon chains that are likely for this structure: polyyne C≡C–C≡C–C or cumulene C═C═C═C. Theoretical calculations tend to suggest that cumulene structures are preferred. At the interface where the carbon chain meets the graphene, the bonding will be more complex, due to the sp^2 nature of graphene meeting the linear carbon chain. Furthermore, under the intense electron beam within a transmission electron microscope (TEM), it is the structures that are "radiation" stable and not those that are "thermodynamically" stable that are imaged.[10]

Using a sample holder that enables *in situ* electrical biasing inside a TEM, the conductivity of these linear carbon chains was recently measured and found to be much lower than predicted for ideal chains.[11] Strain effects were invoked to explain this difference, with calculations suggesting that nonzero strain enables transformations of the carbon chains between cumulene and polyyne configurations. An important aspect to consider when understanding the conductivity of linear carbon chains that interlink graphene is the specific details of how they are bonded to the graphene edges. Under electron-beam irradiation, the linear carbon chains flex and shift their attachment point to graphene, showing surprising robustness under intense irradiation (Figure 2a–d). In Figure 2e,f, the high-magnification TEM images show how the linear C chain bends to accommodate the attachment site. Figure 2g shows a high-resolution TEM image where monochromation of the electron source is used to obtain 80 pm spatial resolution, and in this case, the C atoms appear as sharp spots. The position of atoms in the small linear chain in Figure 2g can be determined from the line

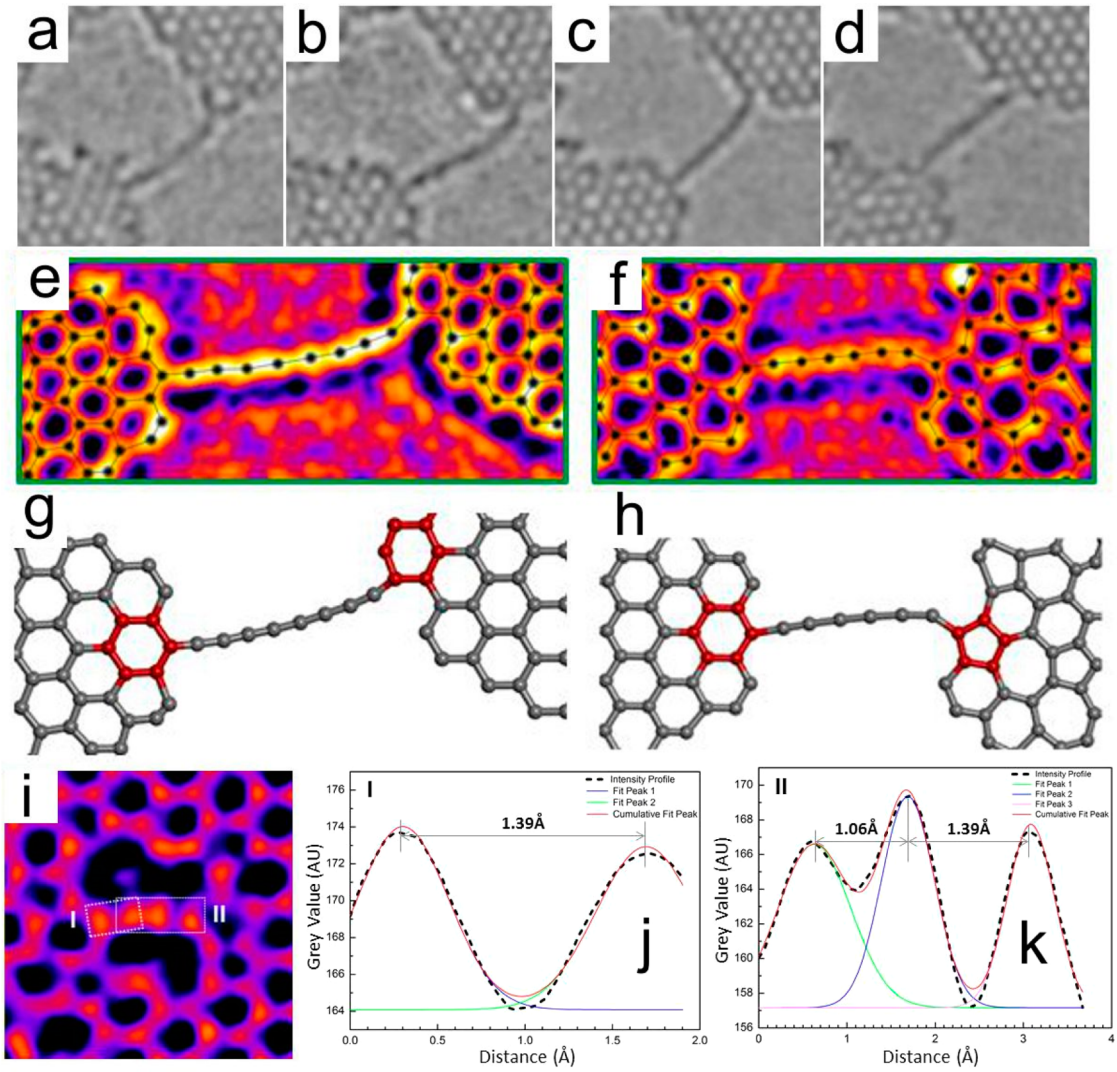

Figure 2. Linear C atomic wires. (a–d) Sequence of AC-TEM images showing the dynamics of a linear C chain within graphene. Time between frames is ~10 s. Area of images is 2.92 × 2.65 nm. (e,f) AC-TEM images (false color) showing the attachment points of two different linear carbon chains at high magnification. Area of images is 3.41 nm × 1.5 nm. (g,h) Atomic models for the AC-TEM images in (e) and (f), respectively. (i) Monochromated AC-TEM image (false color) showing a small C atomic wire in graphene with the position of atoms clearly resolved. Area of image is 1.29 nm × 1.29 nm. (j,k) Box line profiles of the regions indicated with I and II in (i) and include Gaussian fits to measure the C–C bond distances.

profile of the intensity as a function of distance and fitting double Gaussian curves to measure the peak to peak distances (Figure 2j,k), which corresponds to the C–C bond length. Different C–C bond lengths are measured along the chain. The inner C–C bond is shorter than the C–C at the attachment at both ends and confirms that there is a change in both lengths along the linear carbon chains. Linear carbon chain formation has also been found to occur on the surface of graphene, where amorphous carbon monolayers reconstruct under the electron beam and 1D wires interconnect different regions of carbon clusters.[8]

One-Dimensional Atomic Wires in Hexagonal Boron Nitride. With such interesting structural transformations occurring in graphene being directly imaged by AC-TEM, it was only a matter of time before attention was turned to the case of 2D hexagonal boron nitride (h-BN). It is structurally similar to graphene, with a planar hexagonal lattice structure, but with B and N atoms. Hexagonal BN also stacks differently to graphene, with AA′ stacking rather than graphene's AB Bernal stacking (Figure 3). Surprisingly, it has taken 11 years since linear carbon chains were first imaged between nanotubes and 5 years since they were first imaged in graphene, but in this issue of *ACS Nano*, Cretu and coworkers report the first direct experimental confirmation of linear atomic chains within 2D h-BN sheets.[12] Both suspended chains interconnecting regions of BN and chains residing on the surface of BN are imaged with atomic resolution using AC-TEM. The opening of holes in h-BN by electron-beam irradiation has already been studied, but the nanoconstrictions that form when these holes meet and the subsequent atomic wire

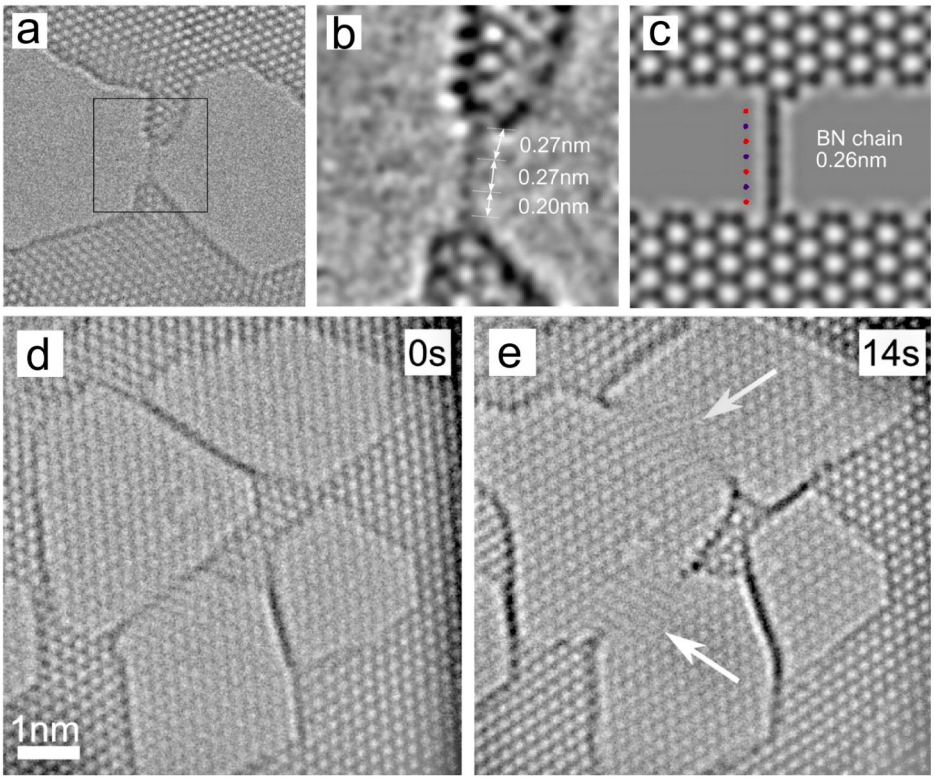

Figure 3. BN atomic wires. (a) AC-TEM image of a suspended linear atomic wire formed in hexagonal boron nitride. Accelerating voltage of 60 kV was used. An *in situ* heating holder was used and set to 650 °C. (b) Region indicated with the black box in (a), processed with a Gaussian blur filter ($r = 2px$) and contrast-enhanced. (c) Multislice image simulation of a BN chain. B and N atoms are inset in blue and red, respectively. (d,e) Two TEM images (14 s apart) showing the atomic chains forming on the surface of h-BN. Data were acquired using 80 kV electrons with the sample at 20 °C. Reprinted from ref 12. Copyright 2014 American Chemical Society.

formation process had not been reported until now. This provides exciting new complementary insights to the work already done on linear carbon chains in graphene. The authors found that the stability and lifetime of the BN chains were enhanced when formed on a supporting BN sheet. The nature of the linear chains was deduced to be heteroatomic, alternating B−N−B-N, *etc.*, through a combination of atomic-resolution AC-TEM and density functional theory calculations. Although calculations indicate that these BN chains are insulating, the structural beauty of their fundamental heteroatomic 1D form will engage the curiosity of a broad range of scientists and stimulate ideas.

Nanowire Formation in Transition Metal Dichalcogenides. The formation of linear 1D atomic wires by electron-beam irradiation is not always a certainty in 2D materials. Recent related electron-beam sputtering experiments on transition metal dichalcogenides reveals that nanowires are formed but not 1D atomic chains (Figure 4).[13,14] However, this might simply be due to the difference in sputtering of S compared to Mo or W. The electron-beam irradiation of Mo- and W-based transition metal dichalcogenides (TMDs) typically leads to the removal of S atoms and the enrichment of Mo or W around the holes.[13] The attachment sites where the nanowires bond to the bulk TMD crystal have higher loading of metal (Figure 4a−d). This is probably why the interconnecting nanowires are metal-rich, with compositions of Mo_5S_4 compared to the starting material, MoS_2 (Figure 4g, h). The formation of Mo_5S_4 under intense electron-beam irradiation is also explained as being due to the higher radiation stability compared to a sulfur-deficient armchair ribbon. Calculations indicate that these sub-1 nm Mo_5S_4 ribbons have a band gap of 0.77 eV.[13]

In this issue of *ACS Nano*, Cretu and coworkers report the first direct experimental confirmation of linear atomic chains within two-dimensional hexagonal boron nitride sheets.

The conductance properties of the nanowires formed in $MoSe_2$ have been explored using an *in situ* electrical biasing holder inside a TEM with surprising results.[14] The conductance of an interconnecting wire was monitored with time, as it gradually decreased in width.

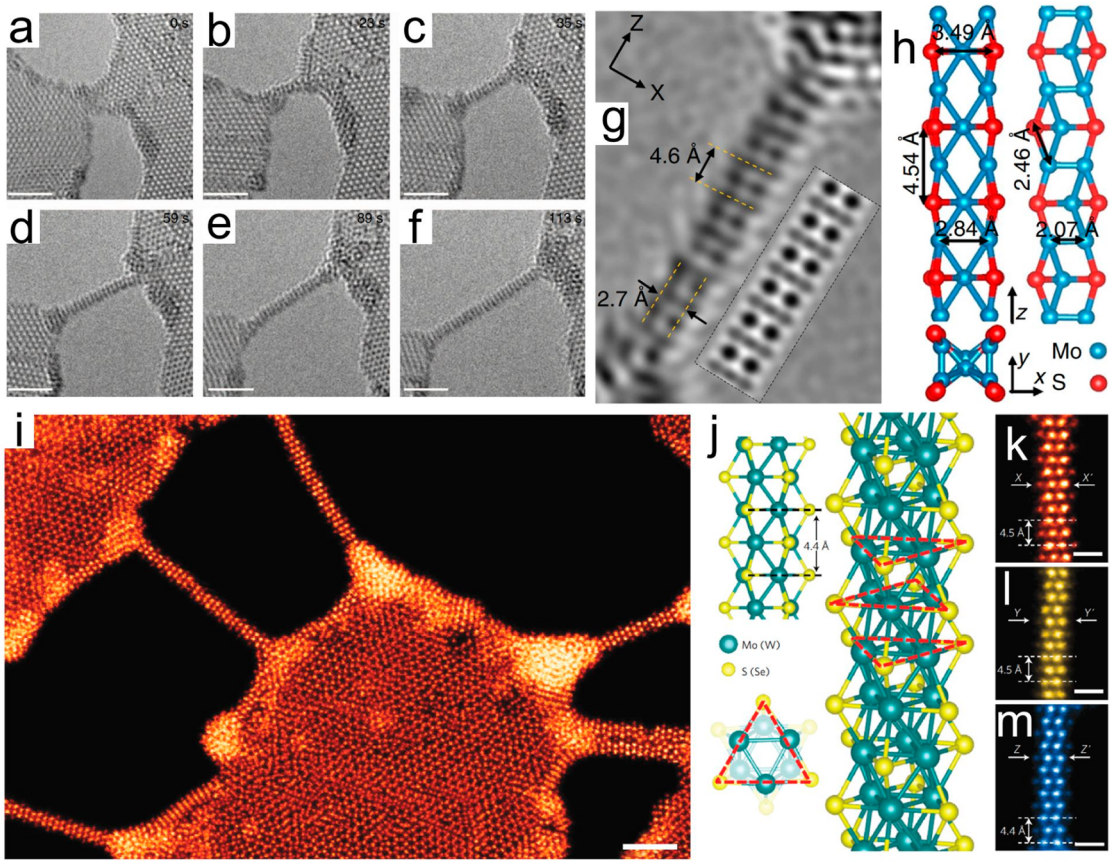

Figure 4. Transition metal dichalcogenide nanowires. (a–f) Sequence of TEM images showing the formation of nanowires in a MoS_2 few-layer flake using an 80 kV electron beam. (g) Comparison between the high-resolution transmission electron microscopy image and simulated TEM image for a Mo_5S_4 nanowire. (h) Atomic models of the Mo_5S_4 ribbon in three different projections. Reproduced with permission from ref 13. Copyright 2013 Nature Publishing Group. (j) Scanning transmission electron microscopy (STEM) *Z*-contrast image (false color) of a patterned MoSe nanowire network, where each nanowire is sculpted individually. Scale bar is 2 nm. (j) Atomic model of the transition metal dichalcogenide nanowire; dashed red triangles indicate the orientation of each layer in the nanowire. (k,l) STEM *Z*-contrast images of individual nanowires from $MoSe_2$ (orange), MoS_2 (yellow), and WSe_2 (blue). Scale bar is 0.5 nm. Reproduced with permission from ref 14. Copyright 2014 Nature Publishing Group.

The initial thick wire (~1 nm) has a dramatic increase in conductance (by an order of magnitude), as the width is reduced by about half; when the wire finally breaks, the conductance drops to zero. The sudden rise in conductance before the wire snaps was attributed to a change from a semiconducting monolayer to a metallic nanowire. As the nanowire shrinks, it will undergo a phase change, which will ultimately lead to modified electrical properties. However, when performing *in situ* biasing experiments inside the TEM, the spatial resolution is impaired and the exact atomic structure of the nanowires is challenging to identify and to link conclusively to predicted properties. As in the cases of atomic wires, interconnected graphene, and h-BN, the MoSe nanowires were also flexible with high degrees of bending regularly observed.[14] Discrete rotations were also seen, enabled by the fact that the wires are thicker than one atom wide and different crystal projections can be identified. Rotation times of the MoSe nanowires were estimated to be on the order of milliseconds and demonstrated self-adaptive reconstruction at the attachment site to the bulk 2D $MoSe_2$.

OUTLOOK AND FUTURE CHALLENGES

With linear atomic chains present in both graphene and h-BN, it will be interesting to see the type of linear chains that might form in 2D hybrids of C–B–N. The linear atomic chains could have several different compositions, such as segmented C and BN or heteroatomic blends of C, B, and N atoms. The merger of C, B, and N elements into linear atomic wires may result in semiconducting behavior, rather than the metallic and insulating forms of C and BN chains alone. A small segment of BN located within the middle of a linear C chain could exhibit interesting transport properties. The effect of single dopant atoms in the linear atomic wires is also an important and interesting factor for bringing electronic diversity to the systems based on C. As the 2D TMDs start to become more integrated with graphene and h-BN, it is worth considering how the nanowires formed in TMDs might interconnect graphene electrodes.

With the progression of 2D materials research pushing toward the isolation and growth of novel 2D materials beyond graphene, BN, and TMDs, there will be many exciting opportunities to explore 1D atomic wire formation in new material systems. Along with graphene, there are other 2D crystals composed of only one element, such as silicene and phosphorene, which have the potential to form monoelement 1D atomic wires. While atomic 1D wires offer tremendous potential in electronics, major challenges in exploiting their properties in large-scale electronics remain. Methods need to be developed that can form 1D interconnecting wires within 2D sheets to develop large-scale arrays and integrated circuits. One possible way this might be achieved is through controlled electrical biasing of graphene (or other material) nanoconstrictions. The biasing of graphene nanoconstrictions can lead to the formation of nanoscale break junctions, and linear carbon chains may also be the penultimate structures before the break junctions form. Using graphene grown by chemical vapor deposition enables several hundred of these devices to be fabricated on one chip with automated processing.[15] By halting the biasing at the right stage, there is a chance that single atomic wires of carbon would be left connecting the two graphene electrodes.

Conflict of Interest: The authors declare no competing financial interest.

REFERENCES AND NOTES

1. Weber, B.; Mahapatra, S.; Ryu, H.; Lee, S.; Fuhrer, A.; Reusch, T. C. G.; Thompson, D. L.; Lee, W. C. T.; Klimeck, G.; Hollenberg, L. C. L.; *et al.* Ohm's Law Survives to the Atomic Scale. *Science* **2012**, *335*, 64–67.
2. Cai, J.; Pignedoli, C. A.; Talirz, L.; Ruffieux, P.; Sode, H.; Liang, L.; Meunier, V.; Berger, R.; Li, R.; Feng, X.; *et al.* Graphene Nanoribbon Heterojunctions. *Nat. Nanotechnol.* **2014**, *9*, 896–900.
3. Warner, J. H.; Ruemmeli, M. H.; Bachmatiuk, A.; Buchner, B. Structural Transformations of Carbon Chains Inside Nanotubes. *Phys. Rev. B* **2010**, *81*, 155419.
4. Kitaura, R.; Imazu, N.; Kobayashi, K.; Shinohara, H. Fabrication of Metal Nanowires in Carbon Nanotubes *via* Versatile Nano-Template Reaction. *Nano Lett.* **2008**, *8*, 693–699.
5. Senga, R.; Komsa, H.-P.; Liu, Z.; Hirose-Takai, K.; Krasheninnikov, A. V.; Suenaga, K. Atomic Structure and Dynamic Behaviour of Truly One-Dimensional Ionic Chains Inside Carbon Nanotubes. *Nat. Mater.* **2014**, *13*, 1050–1054.
6. Warner, J. H.; Margine, E. R.; Mukai, M.; Robertson, A. W.; Guistino, F.; Kirkland, A. I. Dislocation-Driven Deformations in Graphene. *Science* **2012**, *337*, 209–212.
7. Troiani, H. E.; Miki-Yoshida, M.; Camacho-Bragado, G. A.; Marques, M. A. L.; Rubio, A.; Ascencio, J. A.; Jose-Yacaman, M. Direct Observation of the Mechanical Properties of Single-Walled Carbon Nanotubes and Their Junctions at the Atomic Level. *Nano Lett.* **2003**, *3*, 751–755.
8. Chuvilin, A.; Meyer, J. C.; Algara-Siller, G.; Kaiser, U. From Graphene Constrictions to Single Carbon Chains. *New J. Phys.* **2009**, *11*, 083019.
9. Jin, C.; Lan, H.; Peng, L.; Suenaga, K.; Iijima, S. Deriving Carbon Atomic Chains from Graphene. *Phys. Rev. Lett.* **2009**, *102*, 205501.
10. Kotakoski, J.; Santos-Cottin, D.; Krasheninnikov, A. V. Stability of Graphene Edges under Electron Beam: Equilibrium Energetics *versus* Dynamic Effects. *ACS Nano* **2012**, *6*, 671–676.
11. Cretu, O.; Botello-Mendez, A. R.; Janowska, I.; Pham-Huu, C.; Charlier, J.-C.; Banhart, F. Electrical Transport Measured in Atomic Carbon Chains. *Nano Lett.* **2013**, *13*, 3487–3493.
12. Cretu, O.; Komsa, H.-P.; Lehtinen, O.; Algara-Siller, G.; Kaiser, U.; Suenaga, K.; Krasheninnikov, A. V. Experimental Observations of Boron Nitride Chains. *ACS Nano* **2014**, 10.1021/nn5046147.
13. Liu, X.; Xu, T.; Wu, X.; Zhang, Z.; Yu, J.; Qiu, H.; Hong, J.-H.; Jin, C.-H.; Li, J.-X.; Wang, X.-R.; *et al.* Top-Down Fabrication of Sub-nanometre Semiconducting Nanoribbons Derived from Molybdenum Disulfide Sheets. *Nat. Commun.* **2013**, *4*, 1776.
14. Lin, J.; Cretu, O.; Zhou, W.; Suenaga, K.; Prasai, D.; Bolotin, K. I.; Cuong, N. T.; Otani, M.; Okada, S.; Lupini, A. R.; *et al.* Flexible Metallic Nanowires with Self-Adaptive Contacts to Semiconducting Transition-Metal Dichalcogenide Monolayers. *Nat. Nanotechnol.* **2014**, *9*, 436–442.
15. Lau, C. S.; Mol, J. A.; Warner, J. H.; Briggs, G. A. D. Nanoscale Control of Graphene Electrodes. *Phys. Chem. Chem. Phys.* **2014**, *16*, 20398–20401.